

## LETTERS

# The construction of Chasma Boreale on Mars

J. W. Holt<sup>1</sup>, K. E. Fishbaugh<sup>2</sup>, S. Byrne<sup>3</sup>, S. Christian<sup>1,4</sup>, K. Tanaka<sup>5</sup>, P. S. Russell<sup>6</sup>, K. E. Herkenhoff<sup>5</sup>, A. Safaeinili<sup>7,‡</sup>, N. E. Putzig<sup>8</sup> & R. J. Phillips<sup>8</sup>

The polar layered deposits of Mars contain the planet's largest known reservoir of water ice<sup>1,2</sup> and the prospect of revealing a detailed Martian palaeoclimate record<sup>3,4</sup>, but the mechanisms responsible for the formation of the dominant features of the north polar layered deposits (NPLD) are unclear, despite decades of debate. Stratigraphic analyses of the exposed portions of Chasma Boreale—a large canyon 500 km long, up to 100 km wide, and nearly 2 km deep—have led most researchers to favour an erosional process for its formation following initial NPLD accumulation. Candidate mechanisms include the catastrophic outburst of water<sup>5</sup>, protracted basal melting<sup>6</sup>, erosional undercutting<sup>7</sup>, aeolian downcutting<sup>7–9</sup> and a combination of these processes<sup>10</sup>. Here we use new data from the Mars Reconnaissance Orbiter to show that Chasma Boreale is instead a long-lived, complex feature resulting primarily from non-uniform accumulation of the NPLD. The initial valley that later became Chasma Boreale was matched by a second, equally large valley that was completely filled in by subsequent deposition, leaving no evidence on the surface to indicate its former presence. We further demonstrate that topography existing before the NPLD began accumulating influenced successive episodes of deposition and erosion, resulting in most of the present-day topography. Long-term and large-scale patterns of mass balance achieved through sedimentary processes, rather than catastrophic events, ice flow or highly focused erosion, have produced the largest geomorphic anomaly in the north polar ice of Mars.

The NPLD are a sequence of ice-rich layers up to 2 km thick that make up the bulk of Planum Boreum, the overall dome-like structure at the north pole of Mars (Fig. 1a). Chasma Boreale separates the main Planum Boreum lobe from the secondary lobe, Gemina Lingula (Fig. 1a). Beneath approximately 60% of the NPLD<sup>11</sup>, sandy deposits overlie older ice-rich layers<sup>12–14</sup> and together comprise what has been termed the “basal unit”<sup>12</sup>. It has been postulated<sup>12,15</sup> that Chasma Boreale is located along the basal unit's edge in that area, although a causal relationship was not established. Further work has indicated that the floor of Chasma Boreale is probably a residual shelf of lower basal unit<sup>13,16,17</sup>.

Previous observation-based analyses have attempted to deduce Chasma Boreale's history from exposures of stratigraphy at widely spaced outcrops and from landforms existing in its floor. This has led some researchers to conclude that Chasma Boreale was formed as a result of aeolian processes, rather than a basal melt event<sup>8,9,13</sup>. Until recently, however, neither comprehensive NPLD stratigraphy nor large-scale basal topography has been available to construct a full history of Chasma Boreale development or more fully test formation hypotheses. The Mars Reconnaissance Orbiter's SHARAD (SHARAD)<sup>18</sup> now provides this possibility. A SHARAD profile crossing Gemina Lingula (Fig. 1a) and the narrowest part of Chasma

Boreale reveals critical new stratigraphic and structural information (Fig. 2a). As predicted<sup>12</sup> and previously observed<sup>11</sup>, the NPLD within most of Gemina Lingula (radar unit PLD1, Fig. 2b) rest directly on the Vastitas Borealis interior unit<sup>16</sup> which surrounds Planum Boreum<sup>19</sup>. PLD1 layers are subhorizontal, quite uniform in thickness and, based on our mapping of discrete reflectors, can be traced around the head of Chasma Boreale to the opposite side (Supplementary Fig. 1). These radar layers drape the pre-NPLD surface without significant change in thickness and demonstrate that the earliest NPLD deposition was both widespread and uniform.

Higher in the sequence within Gemina Lingula, an angular unconformity truncates subhorizontal radar layers of PLD1 (Fig. 2a, b), implying a depositional hiatus accompanied by erosion. This unconformity extends to the west towards the toe of Gemina Lingula, and to the east where Gemina Lingula merges with the main lobe and beyond (Supplementary Fig. 2). Above this level, remaining NPLD stratigraphy (radar unit PLD2, Fig. 2b) drapes the dome-shaped erosional surface and extends to the floor of Chasma Boreale where Gemina Lingula extends farthest into Chasma Boreale. (Fig. 1a).

The stratigraphic sequence shown in Fig. 2 is sufficient demonstration of the long-term presence of Chasma Boreale, because all layers above the unconformity within Gemina Lingula drape uniformly onto the chasma floor. This validates one prediction of relative longevity<sup>9</sup>, but the stratigraphy also rules out Chasma Boreale formation mechanisms requiring erosion into PLD2 (that is, most of the NPLD). In that case, PLD2 layers would be truncated on both sides of Chasma Boreale and a previous connection could be inferred from their geometry. Additionally, a basal melt event<sup>5,20</sup> or merely enhanced geothermal flux<sup>6</sup> would result in the draw-down of layers in the vicinity of the source. This is not observed in the NPLD stratigraphy preserved adjacent to Chasma Boreale, including near its head, the hypothesized location of such a melt<sup>5</sup> (Supplementary Fig. 1).

Furthermore, we have mapped the evolving Planum Boreum landscape, beginning with the pre-NPLD surface and continuing through major, broad-scale episodes of deposition and erosion, to examine Chasma Boreale formation and development. We first mapped the NPLD base across many SHARAD orbits (Supplementary Fig. 3a). The result (Fig. 1b) agrees well with other recent mapping of the NPLD base with SHARAD<sup>11</sup> and shows that basal unit surface topography is highly non-uniform, especially in the vicinity of present-day Chasma Boreale. This topography seems to have affected the later location of Chasma Boreale: in particular, a low basal-unit scarp coincides with the northern side of the uppermost present-day Chasma Boreale and, together with a lower-relief, disconnected ridge of the basal unit (Figs 1b and 2) detected by SHARAD beneath Gemina Lingula (Gemina Lingula; Fig. 1a), forms a linear depression in the basal unit along the upper half of present-day Chasma Boreale.

<sup>1</sup>Institute for Geophysics, Jackson School of Geosciences, University of Texas at Austin, Austin 78758, Texas, USA. <sup>2</sup>Smithsonian National Air and Space Museum, Washington 20560, District of Columbia, USA. <sup>3</sup>Lunar and Planetary Laboratory, University of Arizona, Tucson 85721, Arizona, USA. <sup>4</sup>Bryn Mawr College, Bryn Mawr 19010, Pennsylvania, USA.

<sup>5</sup>Astrogeology Science Center, US Geological Survey, Flagstaff 86001, Arizona, USA. <sup>6</sup>Planetary Science Institute, Tucson 85719, Arizona, USA. <sup>7</sup>Jet Propulsion Laboratory, Pasadena 91109, California, USA. <sup>8</sup>Southwest Research Institute, Boulder 80302, Colorado, USA.

<sup>‡</sup>Deceased.

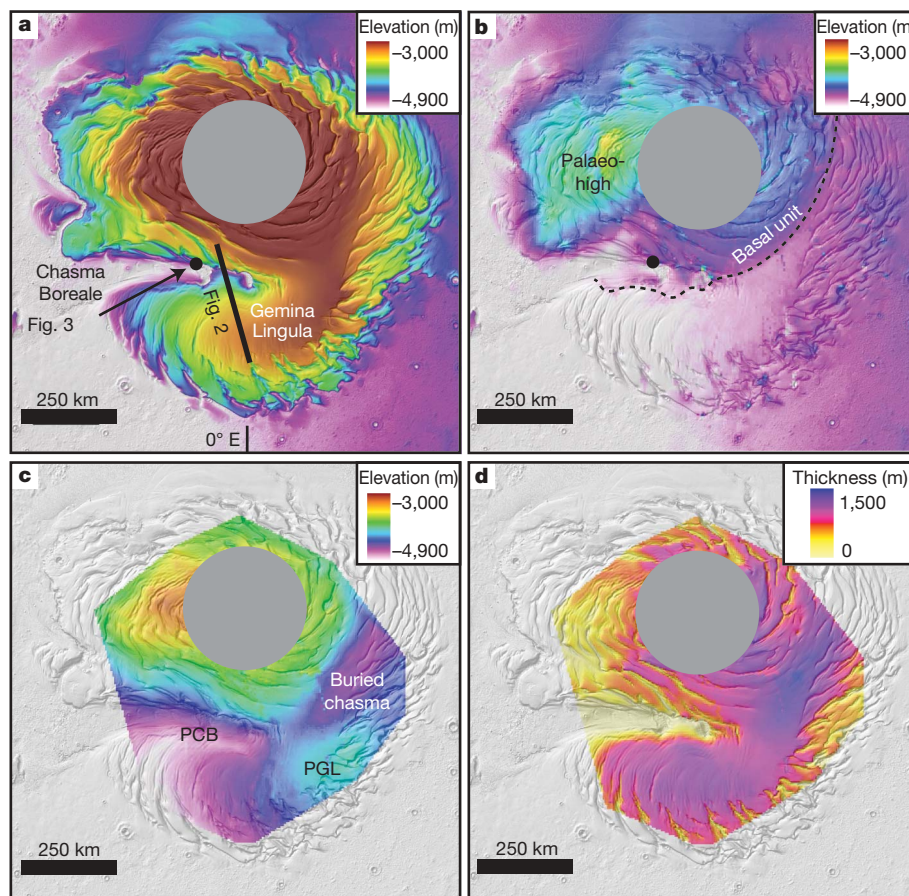


**Figure 1 | Maps of Planum Boreum surface and depositional/erosional history.** **a**, Present surface, based on MOLA data<sup>27</sup> with Chasma Boreale and Gemina Lingula indicated. **b**, Topography of NPLD base as mapped from SHARAD, merged with MOLA surface outside of NPLD. The southern edge of the basal unit beneath NPLD is shown as a dashed line, based on our SHARAD mapping and that of others<sup>11</sup>. The palaeo-high point of the basal surface is indicated. **c**, Topography of unconformity surface at base of PLD2

(Fig. 2b), as mapped using SHARAD data. **d**, Thickness of unit PLD2 (Fig. 2b). For all panels, shading is derived from the present surface, displayed as a semi-transparent overlay in **b–d** for reference. Elevation values are relative to MOLA areoid<sup>27</sup>. See Supplementary Fig. 3 for data coverage used to create gridded surfaces in **b–d**. The gap in coverage from both MOLA and SHARAD north of 87.4° latitude is indicated by the solid grey circle in each panel.

A recently acquired image (Fig. 3) from the High Resolution Imaging Science Experiment (HiRISE) camera<sup>21</sup> on the Mars Reconnaissance Orbiter further clarifies how the NPLD contacts the basal unit in the area of Chasma Boreale. Here the lowest NPLD layers, corresponding to radar unit PLD1, clearly drape a scarp eroded into the upper (cavi<sup>13</sup>) unit of the basal unit. This scarp forms part of the wall of Chasma Boreale, so its superposition by these layers demonstrates that initial NPLD deposition post-dated erosion of at least the upper basal unit along the northern margin of Chasma Boreale. The cavi–NPLD contact is gradational or laterally transgressive in other locations<sup>13</sup>, indicating that the erosion seen here immediately predates NPLD deposition and was localized, perhaps helping to reinforce or create a nascent Chasma Boreale depression. As indicated by previous geologic mapping<sup>13</sup>, this erosion is distinct from the much earlier erosion of the lower (Rupes Tenuis<sup>13</sup>) part of the basal unit that is responsible for most of the strong basal relief that we have mapped. The pre-NPLD landscape includes a major scarp striking north–south, located between the present-day Chasma Boreale and the most significant basal unit palaeo-high (Fig. 1b). This scarp may have acted as a regional control on later deposition and erosion, as our further mapping suggests.

To evaluate subsequent patterns of NPLD deposition and erosion, we mapped the PLD1–PLD2 contact across Planum Boreum using many intersecting SHARAD orbits (Supplementary Fig. 3b). In contrast to recent SHARAD mapping of Planum Boreum that delineated packets of radar-bright and radar-dark zones<sup>11</sup>, our effort focused on a discrete stratigraphic level representing a depositional hiatus, indicated

by the radar reflector draping the angular unconformity within Gemina Lingula (Fig. 2) and elsewhere (Supplementary Fig. 2). This now-buried landscape (Fig. 1c) includes an elongated dome almost entirely separated from the polar topographic high, a proto-Gemina Lingula (PGL; Fig. 1c), and two broad, deep valleys, one that is essentially a proto-Chasma Boreale (PCB; Fig. 1c) the axis of which is offset to the east of the present-day Chasma Boreale, and another, equally large valley to the east (Fig. 1c).

How did this landscape develop? Given that PLD1 deposition was quite uniform, as indicated by subhorizontal and parallel radar layering throughout, widespread erosion must have occurred throughout the entire region of PGL, PCB and the buried chasma to produce the long-wavelength topography observed. (Supplementary Fig. 4 shows the pattern of net accumulation thickness resulting from PLD1 deposition and subsequent erosion.) The arcuate shape of PGL (where erosion was most prevalent) and its location adjacent to and south of the main lobe (Fig. 1c) further suggest that katabatic winds descending from the polar high played a part, perhaps along with solar ablation.

The comparison of the unconformity palaeosurface (Fig. 1c) with today's surface (Fig. 1a) reveals that non-uniform deposition of PLD2 material resulted in significant changes in the landscape. A thickness map of unit PLD2 (Fig. 1d) shows that most deposition subsequent to the unconformity was concentrated in the PGL–buried chasma region (at least below the 87.4° N limit of SHARAD and MOLA data). Whereas the buried chasma was completely filled in with up to 1.5 km of material, PCB became longer and narrower owing to the deposition

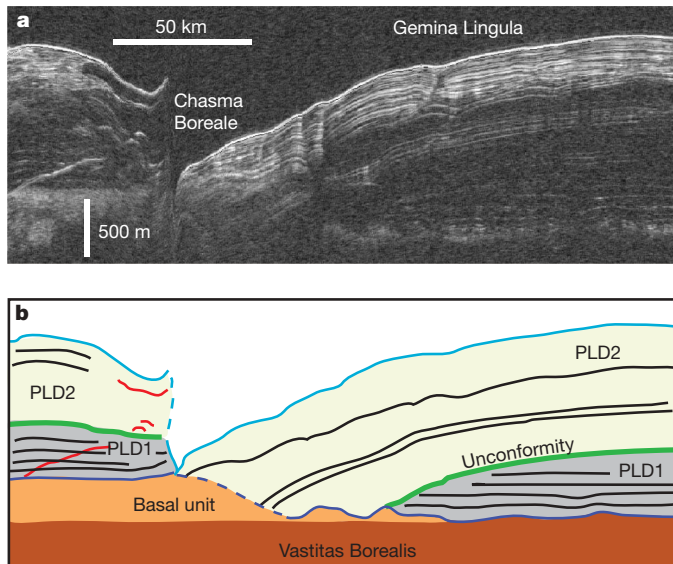


**Figure 2 | SHARAD data and interpretation.** **a**, Depth-corrected radargram crossing Chasma Boreale (portion of SHARAD observation 522402. See Fig. 1a for location). Vertical exaggeration is about 45:1. **b**, Interpretation of stratigraphy and geologic units, showing representative radar reflectors and the unconformity surface. Unit designations PLD1 and PLD2 are based on radar data and do not necessarily correspond to previously mapped geologic units. Boundaries are dashed where inferred. The Vastitas Borealis interior unit<sup>13</sup> is assumed to underlie the basal unit or PLD1 where the basal unit is not present within Gemina Lingula. The base of the basal unit is generally not detectable with SHARAD, but the basal unit itself is distinctive owing to strong volume scattering causing an increased amount of dispersed energy. Red lines indicate off-nadir surface echoes (clutter), as determined by simulations.

of about a kilometre of PLD2 draping PGL (Fig. 1c, d) and extending farther to the east. An asymmetrical cross-section across PCB (higher and steeper slopes to the north, lower and shallower slopes to the south) must have been maintained throughout this phase, as indicated by the geometry and proximity of layers shown in Fig. 2. The strong topographic relief northwest of PCB (towards the palaeo-high in Fig. 1c) may have played a critical role in this asymmetry, enhancing the strength of katabatic winds descending from the polar high and preventing accumulation along the axis of PCB. By contrast, total relief on the northern side of the buried chasma was significantly less (Fig. 1c), perhaps enabling deposition to outpace the effect of katabatic winds there, resulting in the complete infilling of the buried chasma.

The dome-like cross-section of the PGL was largely maintained in this later depositional stage, leading to today's Gemina Lingula

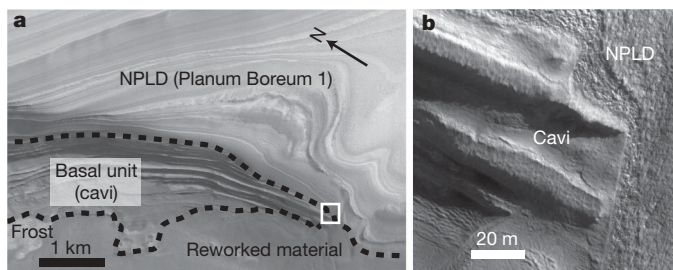


**Figure 3 | HiRISE image PSP\_009914\_2750 showing depositional relationship between NPLD and basal unit.** Illumination from upper right. **a**, Unconformable contact between lowest NPLD unit (Planum Boreum 1 unit<sup>13</sup>) and the uppermost basal unit (cavi unit<sup>13</sup>) on the north margin of Chasma Boreale. Contact, indicated by the upper dotted line, is obscured on the right side by recent deposition of reworked material, the uppermost extent of which is indicated by the lower dotted line. See Fig. 1a for location. **b**, Close-up view of NPLD-basal unit contact, location indicated by box in **a**.

(Fig. 1a, c, d and Fig. 2). Examining SHARAD data down-chasma of the radar profile shown in Fig. 2, we find that the upper PLD2 layers within Gemina Lingula are truncated along the Chasma Boreale margin (Supplementary Fig. 5), indicating that the lower section of Chasma Boreale did experience erosion after the most recent stage of NPLD deposition. The entire sequence of events leading to the development of this cross-sectional view of Chasma Boreale, taking into account information that we gleaned from the HiRISE image and pan-NPLD mapping with SHARAD, is illustrated schematically in Fig. 4. Briefly, strong erosion of the basal unit (Fig. 4a, b) is followed by uniform deposition (Fig. 4c), then large-scale erosion resulting in a dome distinct from the main lobe (Fig. 4d), followed by an additional phase of deposition draping the dome and the main lobe (Fig. 4e), and a final stage of recent erosion (Fig. 4f) that steepened many slopes and widened Chasma Boreale in its lower section.

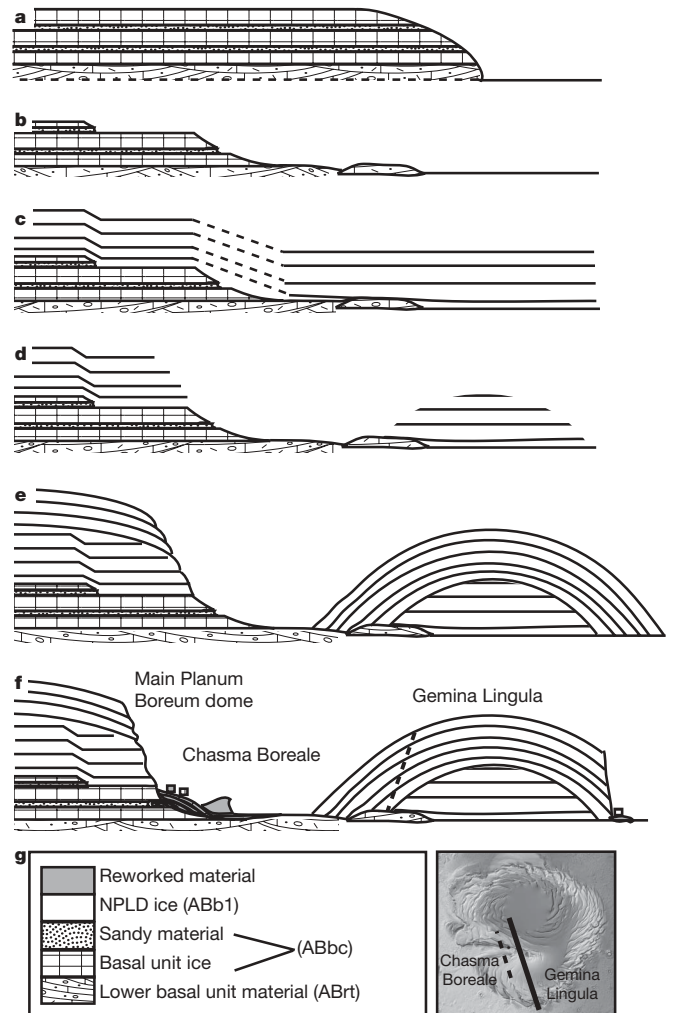


**Figure 4 | Cross-sectional illustration of hypothesized sequence of events leading to the development of Chasma Boreale and Gemina Lingula.** The figure is based on data presented in Figs 1–3 and Supplementary Figs 1–5. The location is indicated by solid line in map view (**g**); it is approximately the same location as Fig. 2. **a**, Basal unit before modification. **b**, Erosion of the basal unit. **c**, Deposition of radar unit PLD1. Presumed deposition across location of present-day Chasma Boreale shown as dashed lines. **d**, Erosion of PLD1. **e**, Deposition of radar unit PLD2. **f**, Recent erosion of NPLD increasing steepness of most slopes. Dashed near-vertical line shows erosion of PLD2 farther west (dashed line on map in **g**; see Supplementary Fig. 5 for examples of radar data). ABrt, ABbc and ABb1 are, respectively, the Rupes Tenuis, Planum Boreum cavi, and Planum Boreum 1 units, as defined in ref. 13.

Our findings show that in spite of the overall uniform appearance of NPLD stratigraphy, non-uniform accumulation patterns with probable control from initial surface relief and continued topographic feedback have produced Chasma Boreale, the largest single anomaly of the northern polar ice of Mars. A similar process has been suggested to explain the southern polar chasmata, based on mapping of surface exposures<sup>22</sup>. Other findings<sup>23</sup> show likewise that the spiral-shaped troughs of the NPLD have formed and evolved during a geologically recent period of net accumulation, as opposed to erosion as generally assumed. The preservation of complex structures including major angular unconformities indicates that sedimentary processes such as deposition, erosion and lateral transport have been the primary factors determining the nature of polar stratigraphy of Mars, unlike on the Earth, where ice flow leaves a pervasive impact on layering. The stratigraphic record, in turn, supports long-term and large-scale processes (that is, obliquity-driven climate change and a quasi-periodic global redistribution of water ice) as the primary controls in shaping the polar ice of Mars, rather than highly focused and possibly catastrophic events.

### METHODS SUMMARY

Theoretical<sup>24</sup> and empirical<sup>25</sup> studies indicate that radar reflections result from contrasts in the dielectric properties of visible NPLD layers and therefore serve to represent the same geometrical relationships. Depth conversion of SHARAD data assumes a permittivity (real part) of 3.15, equivalent to that of pure water ice and consistent with a value determined empirically for Gemina Lingula<sup>26</sup>. In SHARAD data, the basal unit can typically be distinguished from the NPLD owing to its significant volume scattering and lack of internal reflectors<sup>2,11</sup>. Radar reflectors and contacts were traced across multiple intersecting lines using Schlumberger Corporation's GeoFrame seismic data interpretation software. Resulting positions in time delay were georeferenced and gridded into surfaces using ESRI's ArcGIS after conversion to depth and alignment with surface elevations determined from the Mars Orbiter Laser Altimeter<sup>27</sup> to determine absolute elevations of internal layers.

Received 17 December 2009; accepted 10 March 2010.

1. Plaut, J. J. *et al.* Subsurface radar sounding of the south polar layered deposits of Mars. *Science* **316**, 92–95 (2007).
2. Phillips, R. J. *et al.* Mars north polar deposits: stratigraphy, age, and geodynamical response. *Science* **320**, 1182–1185 (2008).
3. Byrne, S. The polar deposits of Mars. *Annu. Rev. Earth Planet. Sci.* **37**, 8.1–8.26 (2009).
4. Clifford, S. M. *et al.* The state and future of Mars polar science and exploration. *Icarus* **144**, 210–242 (2000).
5. Clifford, S. M. Chasma Boreale (85°N, 0°W): remnant of a Martian jokulhlaup? *Bull. Am. Astron. Soc.* **12**, 678–679 (1980).
6. Greve, R. Scenarios for the formation of Chasma Boreale, Mars. *Icarus* **196**, 359–367 (2008).
7. Edgett, K. S., Williams, R. M. E., Malin, M. C., Cantor, B. A. & Thomas, P. C. Mars landscape evolution: influence of stratigraphy on geomorphology in the north polar region. *Geomorphology* **52**, 289–297 (2003).
8. Warner, N. H. & Farmer, J. D. Importance of aeolian processes in the origin of the north polar chasmata, Mars. *Icarus* **196**, 368–384 (2008).
9. Howard, A. D. The role of eolian processes in forming surface features of the Martian polar layered deposits. *Icarus* **144**, 267–288 (2000).
10. Fishbaugh, K. E. & Head, J. W. III. Chasma Boreale, Mars: topographic characterization from Mars Orbiter Laser Altimeter data and implications for mechanisms of formation. *J. Geophys. Res.* **107** (E3), doi: 10.1029/2000JE001351 (2002).

11. Putzig, N. E. *et al.* Subsurface structure of Planum Boreum from Mars Reconnaissance Orbiter shallow radar soundings. *Icarus* **204**, 443–457 (2009).
12. Byrne, S. & Murray, B. C. North polar stratigraphy and the paleo-erg of Mars. *J. Geophys. Res.* **107** (E6), doi: 10.1029/2001JE001615 (2002).
13. Tanaka, K. L. *et al.* North polar region of Mars: advances in stratigraphy, structure, and erosional modification. *Icarus* **196**, 318–358 (2008).
14. Herkenhoff, K. E., Byrne, S., Russell, P. S., Fishbaugh, K. E. & McEwen, A. S. Meter-scale morphology of the north polar region of Mars. *Science* **317**, 1711–1715 (2007).
15. Fishbaugh, K. E. & Head, J. W. Origin and characteristics of the Mars north polar basal unit and implications for polar geologic history. *Icarus* **174**, 444–474 (2005).
16. Tanaka, K. L. Geology and insolation-driven climatic history of Amazonian north polar materials on Mars. *Nature* **437**, 991–994 (2005).
17. Kolb, E. J. & Tanaka, K. L. Geologic history of the polar regions of Mars based on Mars Global Surveyor data. II. Amazonian period. *Icarus* **154**, 22–39 (2001).
18. Seu, R. *et al.* SHARAD sounding radar on the Mars Reconnaissance Orbiter. *J. Geophys. Res.* **112**, E05S05 (2007).
19. Tanaka, K. L. *et al.* *Geologic Map of the Polar Regions of Mars* USGS Misc. Map Series, Map I-1802-C (USGS, 1987).
20. Clifford, S. M. Polar basal melting on Mars. *J. Geophys. Res.* **92**, 9135–9152 (1987).
21. McEwen, A. S. *et al.* Mars Reconnaissance Orbiter's High Resolution Imaging Science Experiment (HiRISE). *J. Geophys. Res.* **112** (E5), doi: 10.1029/2005JE002605 (2007).
22. Kolb, E. J. & Tanaka, K. L. Accumulation and erosion of south polar layered deposits in the Promethei Lingula region, Planum Australe, Mars. *Mars J.* **2**, 1–9 (2006).
23. Smith, I. B. & Holt, J. W. Onset and migration of spiral troughs on Mars revealed by orbital radar. *Nature* doi: 10.1038/nature09049 (this issue).
24. Nunes, D. C. & Phillips, R. J. Radar subsurface mapping of the polar layered deposits on Mars. *J. Geophys. Res.* **111**, E06S21 (2006).
25. Milkovich, S. M. *et al.* Stratigraphy of Promethei Lingula, south polar layered deposits, Mars, in radar and imaging data sets. *J. Geophys. Res. Planets* **114**, E03002 (2009).
26. Grima, C. *et al.* North polar deposits of Mars: extreme purity of the water ice. *Geophys. Res. Lett.* **36**, L03203, doi:10.1029/2008GL036326 (2009).
27. Smith, D. E. *et al.* Mars Orbiter Laser Altimeter: experiment summary after the first year of global mapping of Mars. *J. Geophys. Res.* **106**, 23689–23722 (2001).

**Supplementary Information** is linked to the online version of the paper at [www.nature.com/nature](http://www.nature.com/nature).

**Acknowledgements** We thank P. Choudhary for assistance with radar data analysis. Work at the University of Texas was supported by the Institute for Geophysics of the Jackson School of Geosciences, a NASA grant (NAG5-12693) to J.W.H. and a Mars Reconnaissance Orbiter (MRO) Participating Scientist grant to J.W.H. MRO is operated for NASA by Caltech's Jet Propulsion Laboratory. SHARAD was provided to MRO by the Italian Space Agency through a contract with Thales Alenia Space Italia, and is operated by the INFOCOM Department, University of Rome. We thank the SHARAD Operations Center in Rome for their critical support. We honour the memory of our co-author and colleague A.S. This is UTIG contribution number 2186.

**Author Contributions** J.W.H. initiated and led the SHARAD analysis effort, synthesized results and wrote the manuscript. K.E.F. and S.B. led HiRISE analysis, contributed material for early manuscript drafts and assisted in the final manuscript. S.C. assimilated SHARAD data and performed most of the radar mapping. A.S. provided focused and depth-corrected SHARAD data. K.T., K.E.H. and P.S.R. contributed to the HiRISE analysis and the manuscript. N.E.P. and R.J.P. provided radar validation and contributed to the manuscript.

**Author Information** Data from MRO, including SHARAD and HiRISE, are available at NASA's Planetary Data System (<http://pds.jpl.nasa.gov/>). Reprints and permissions information is available at [www.nature.com/reprints](http://www.nature.com/reprints). The authors declare no competing financial interests. Readers are welcome to comment on the online version of this article at [www.nature.com/nature](http://www.nature.com/nature). Correspondence and requests for materials should be addressed to J.W.H. ([jack@ig.utexas.edu](mailto:jack@ig.utexas.edu)).